

ORIGINAL ARTICLE

The Utility of a Combination of ^{99m}Tc -MIBI Washout Imaging and Cardiac Magnetic Resonance Imaging in the Evaluation of Cardiomyopathy

Moriaki Yamanaka, MD¹⁾, Shoichiro Takao, MD, PhD²⁾, Hideki Otsuka, MD, PhD³⁾, Yoichi Otomi, MD, PhD¹⁾, Saho Irahara, MD¹⁾, Yamato Kunikane, RT⁴⁾, Satoru Takashi, RT⁴⁾, Airi Yamamoto, RT⁵⁾, Masataka Sata, MD, PhD⁶⁾ and Masafumi Harada, MD, PhD¹⁾

Received: May 29, 2020/Revised manuscript received: April 19, 2021/Accepted: April 27, 2021

J-STAGE advance published: June 25, 2021

© The Japanese Society of Nuclear Cardiology 2021

Abstract

Background: In cardiomyopathy, ^{99m}Tc -MIBI washout can reflect mitochondrial dysfunction and late gadolinium enhancement (LGE) on cardiac magnetic imaging (MRI) is associated with tissue fibrosis. We sought to determine the relationship between ^{99m}Tc -MIBI uptake, ^{99m}Tc -MIBI washout, and LGE on MRI in patients with cardiomyopathy.

Methods: Twenty-one patients underwent rest myocardial perfusion scintigraphy at 45 minutes (early) and 4 hours (delayed) after intravenous ^{99m}Tc -MIBI administration and cardiac MRI. We assessed myocardial perfusion, ^{99m}Tc -MIBI washout, and LGE. We divided the left ventricle (LV) wall into 16 segments using a polar map. Then, we classified each segment into 5 groups according to ^{99m}Tc -MIBI uptake in early-rest images and washout. Additionally, we created a contingency table based on LGE presence/absence in the groups.

Results: We evaluated 336 segments in 21 patients. ^{99m}Tc -MIBI uptake was decreased in 168 segments in the early-rest ^{99m}Tc -MIBI images. ^{99m}Tc -MIBI washout was observed in 108 segments with either normal perfusion or reduced perfusion in the early-rest ^{99m}Tc -MIBI images. LGE was positive in 104 segments. A contingency table analysis with Fisher's exact test showed that LGE was observed significantly more frequently in the segments with decreased ^{99m}Tc -MIBI uptake ($p < 0.001$). In segments without a decreased ^{99m}Tc -MIBI uptake, there was a significant correlation between increased ^{99m}Tc -MIBI washout and the presence of LGE ($p = 0.033$).

Conclusions: In cardiomyopathy, the mitochondrial dysfunction in the early stage is shown as ^{99m}Tc -MIBI washout, and fibrotic changes in the myocardium in advanced stages are shown as LGE on cardiac MRI. The severity of myocardial damage and the clinical stage of cardiomyopathy can be evaluated using multimodal imaging.

Keywords: ^{99m}Tc -MIBI, Cardiomyopathy, Late gadolinium enhancement (LGE), Washout

Ann Nucl Cardiol 2021; 7 (1): 8–16

Cardiomyopathy is associated with several kinds of myocardial injury. Radionuclide studies and cardiac magnetic resonance imaging (MRI) can evaluate myocardial impairment and cardiac function; they play important roles in cardiomyopathy diagnosis.

^{99m}Tc -methoxy-isobutyl-isonitrile (^{99m}Tc -MIBI) is a widely used perfusion radiotracer for coronary artery disease detection. ^{99m}Tc -MIBI is taken up by passive diffusion as cations into cardiomyocytes and subsequently into the negatively charged mitochondria (1). The myocellular uptake

doi: 10.17996/anc.21-00124

1) Department of Radiology, Tokushima University Hospital, Tokushima, Japan

2) Department of Diagnostic Radiology, Graduate School of Biomedical Sciences, Tokushima University, Tokushima, Japan

3) Department of Medical Imaging/Nuclear Medicine, Graduate School of Biomedical Sciences, Tokushima University, Tokushima, Japan

4) Division of Clinical Technology, Tokushima University Hospital, Tokushima, Japan

5) Department of Radiology, Takamatsu Municipal Hospital, Kagawa, Japan

6) Department of Cardiovascular Medicine, Graduate School of Biomedical Sciences, Tokushima University, Tokushima, Japan

and retention of MIBI are strongly dependent on the mitochondrial and plasma membrane potentials, both qualitatively and quantitatively (1). In damaged cardiomyocytes, the mitochondria's negative membrane potential becomes smaller, and the potential difference with cations decreases. As a result, ^{99m}Tc -MIBI uptake is reduced, and retention in the myocardium decreases. ^{99m}Tc -MIBI is then released outside of the myocardium, and washout increases. Previous studies have shown that restriction of ^{99m}Tc -MIBI myocardial uptake is associated with ongoing myocardial damage (2, 3). Additionally, the increase in ^{99m}Tc -MIBI washout may suggest altered mitochondrial function or mitochondrial dysfunction (4, 5). However, the significance of evaluating ^{99m}Tc -MIBI washout for clinical diagnosis of cardiomyopathy remains unclear.

Cardiac MRI is considered a gold standard modality for noninvasive myocardial function assessment and can visualize and quantify scarring using late gadolinium enhancement (LGE) (6). LGE regions are defined as necrotic or fibrotic regions caused by prolonged retention of gadolinium, compared with normal regions.

Previous reports have shown that LGE is a useful and reproducible method for assessing myocardial fibrosis in patients with cardiomyopathy (7–9). Furthermore, some reports have revealed a relationship between a decrease in ^{99m}Tc -MIBI uptake and LGE (10, 11). However, the relationship between ^{99m}Tc -MIBI washout and LGE in cardiomyopathy has not been well characterized.

We hypothesized that ^{99m}Tc -MIBI washout, which is thought to reflect mitochondrial dysfunction, may help assess earlier myocardial damage than LGE, which is thought to reflect fibrosis. We investigated the relationship between the presence or absence of ^{99m}Tc -MIBI uptake abnormality, increased ^{99m}Tc -MIBI washout, and LGE. Further, this study determined whether the presence of ^{99m}Tc -MIBI washout was significantly associated with myocardial fibrosis, as detected by MRI in patients with cardiomyopathy. Moreover, we sought to determine the relationship between ^{99m}Tc -MIBI uptake, ^{99m}Tc -MIBI washout, and LGE on cardiac MRI in patients with cardiomyopathy.

Materials and methods

Study population

We included 25 patients with cardiomyopathy who presented to us between January 2011 and November 2017. These patients showed early and delayed-rest myocardial perfusion imaging (MPI) on ^{99m}Tc -MIBI (FUJI-Toyama RI Pharma, Tokyo, Japan) and gadolinium-enhanced cardiac MRI. MRI was performed within an average of 13 days (range: 0–26 days) using ^{99m}Tc -MIBI scintigraphy. All patients were >18 years and clinically diagnosed with cardiomyopathy.

No patient had received drugs for cardiomyopathy, such as steroids, before the examination, and none had undergone any intervention, such as pacemaker implantation or surgery before examination. All patients underwent coronary angiography. No patient showed significant coronary stenosis. This study was approved by Tokushima University Hospital's Institutional Review Board and Ethics Committee. The need for written informed consent was waived.

^{99m}Tc -MIBI protocol

Rest imaging protocol was 45 minutes (early) and 4 hours (delayed) after intravenous administration of 370–500 MBq of ^{99m}Tc -MIBI (2, 12). The patient was asked to ingest a chocolate bar or milk before imaging to reduce artifacts associated with abdominal accumulation. Data acquisition was performed using a dual-head gamma camera (E. CAM; Toshiba Medical Corporation Systems, Odawara, Japan). For each image, electrocardiogram-gated single-photon emission computed tomography (SPECT) was conducted following planar imaging. The ^{99m}Tc -MIBI scan protocol and parameters included: in planar images: matrix size, 256×256 ; magnification, 1.00; collecting time, 3 minutes front, 3 minutes lateral; in SPECT images: matrix size, 64×64 ; magnification, 1.78, step and shoot, non-circular orbit, 30 views; collection time, 30 seconds per view; rotary angle, 180° ; scan duration, 900 seconds; reconstruction via the ordered subset expectation maximization method, and Gaussian filter.

^{99m}Tc -MIBI data analyses

Image reconstruction

The cardiac function analysis software program CardioBull (Fujifilm RI Pharma Co., Ltd., Tokyo, Japan) was used for the analysis of SPECT images. By importing the short-axis images into the program, the optimal apical and basal slices were automatically determined. For qualitative polar map creation, automatic co-registration was applied for pairs of short-axis images (13). A myocardial perfusion polar map was generated using a circumferential profile curve analysis with the apical radial sampling method (14). LV wall was divided into 17 segments (15) (Figure 1a).

Image interpretation

A double-board-certified physician, H. O. (diagnostic radiology and nuclear medicine), evaluated the ^{99m}Tc -MIBI images visually in this study. We applied a 5-point visual scale to each segment (defect score; 0: normal uptake, 1: mildly decreased, 2: moderately decreased, 3: severe decreased, 4: perfusion defect) in the early and delayed-rest images (2, 12). We evaluated the washout by scoring and judging the uptake in the early- and delayed-rest images and comparing the two; we considered an increase of one or more segmental defect scores (2, 12).

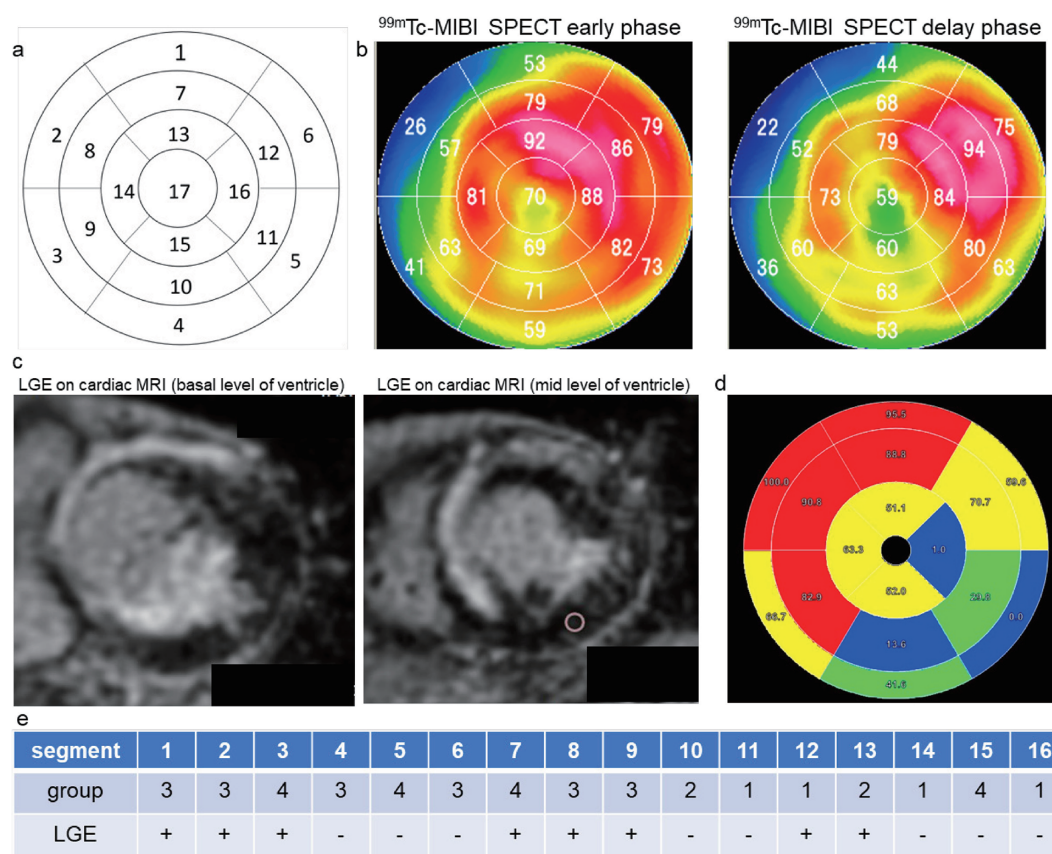


Figure 1 ^{99m}Tc -MIBI SPECT and MRI analyses.

a: left ventricular wall was divided into 17 segments.

b: ^{99m}Tc -MIBI SPECT in the early and delayed phase.

c: LGE on MRI at the basal and mid-level of the left ventricle.

d: Polar map showing LGE spread in each segment analyzed by Ziostation.

e: Summary of analysis results.

Segmental Classification

We defined a defect score 0 as normal uptake and defect score 1–4 as abnormal uptake in the early-rest images. The subjects were classified into the following five groups based on ^{99m}Tc -MIBI uptake in the early-rest images and presence or absence of ^{99m}Tc -MIBI washout: Group 1, normal uptake without ^{99m}Tc -MIBI washout; Group 2, normal uptake with washout; Group 3, abnormal uptake without washout; Group 4, abnormal uptake with washout; Group 5, abnormal uptake and fill-in (Figure 1b and e).

Cardiac MRI

Cardiac MRI was performed with a 1.5-T MRI scanner (GE Signa Excite 1.5 T; General Electric, Milwaukee, WI, USA) using a phased-array coil. All cardiac MR images were electrocardiographically gated and obtained during repeated breath-holds. To evaluate the left ventricle's anatomy, short-axis images, and two-, three-, and four-chamber long-axis views were obtained by cine-MRI, using a steady-state free-precession technique. Gadopentetate meglumine (0.15 mmol/kg; Magnevist; Schering AG, Berlin, Germany) was then administered at a rate of 3–4 mL/s using a power injector.

LGE images were acquired 10 min after injection of gadopentetate meglumine, with an inversion-recovery SSFP pulse sequence and inversion time of 300 ms. Image parameters were as follows: repetition time (TR), 5.8 ms; excitation time (TE), 2.3 ms; image matrix, 256×128 ; field of view, 360 mm; slice thickness, 10 mm; spacing, 2–4 mm; flip angle, 12° ; and k-space/cardiac cycle, 8–12 lines. Images were acquired during short breath-holding (12–15 seconds) at end inspiration (16).

Cardiac MRI data analyses

We analyzed the LGE images using the Ziostation 2 software program (Ziosoft, Tokyo, Japan). Short-axis LGE images were used for the analysis. We excluded the apex and base segments as these sections' scans did not include the left ventricle muscle or the beveled myocardium, which may have caused incorrect signal intensities. LGE regions were automatically defined as those exhibiting a signal intensity above a predetermined threshold. We used a threshold of five standard deviations (SD) above the signal intensity of the non-damaged myocardium, as LGE quantification with this threshold showed the best agreement with the visual

Table 1 Patients' characteristics

Parameter	Data
Gender (n), male/female	13/8
Age (years) mean \pm SD/range	60 \pm 13 (28-82)
Body weight (Kg) mean \pm SD/range	62.9 \pm 17.7 (41-100)
Cardiac function indices	
End-diastolic volume (ml) mean \pm SD/range	146.5 \pm 69.6 (64-254)
End-systolic volume (ml) mean \pm SD/range	80.5 \pm 56.4 (22-166)
Ejection fraction (%) mean \pm SD/range	49.4 \pm 15.5 (26-72)
Type of cardiomyopathy	
Sarcoidosis/hypertensive/DCM/takotsubo/HCM/toxic	8/5/4/2/1/1

The cardiac function indices were calculated by quantitative gated single-photon emission computed tomography.

DCM: dilated cardiomyopathy, HCM: hypertrophic cardiomyopathy, Hypertensive: hypertensive cardiomyopathy, Sarcoidosis: cardiac sarcoidosis, SD: standard deviation, Takotsubo: takotsubo cardiomyopathy, toxic: toxic cardiomyopathy

Table 2 Relationship between ^{99m}Tc -MIBI washout and LGE

	LGE negative	LGE positive	Total
Washout negative	163 (71.5%)	65 (28.5%)	228
Washout positive	69 (63.9%)	39 (36.1%)	108

LGE: late gadolinium enhancement

MIBI: ^{99m}Tc -methoxy-isobutyl-isonitrile

Fisher's exact test: $p=0.165$

assessment and the best reproducibility among different techniques thresholds (17). The results were shown as a polar map divided into 16 segments. We excluded the apex from the standard 17-segment model, as the apex cannot be assessed in short-axis LGE images. The extent of LGE was calculated as the area ratio (%) for each segment. In this study, the qualitative evaluation was performed as with the analysis of ^{99m}Tc -MIBI. Positive LGE was defined as an extent of $\geq 60\%$ LGE in the segment. Negative LGE was defined as an extent $< 60\%$ (Figure 1c-e).

Statistical analyses

Continuous variables are expressed as mean \pm standard deviation. Categorical variables are described as numbers and percentages. The Kolmogorov-Smirnov test was used to evaluate the normality of the data distribution. The data of each segment were considered as independent qualitative data, and their consistency was examined. Fisher's exact test was used to examine differences in proportion (categorical variables). These statistical analyses were performed with IBM SPSS Statistics 23 software program for Windows (IBM Corp., Armonk, NY, USA). Statistical significance was set at $p < 0.05$.

Results

Patients' characteristics

Among the 25 patients, four patients we excluded because of poor MRI image quality due to motion artifacts. Therefore, only 21 patients were analyzed. Patient characteristics are shown in Table 1. Patients' clinical diagnoses were classified as idiopathic or specific cardiomyopathy, according to Japanese guidelines (18).

Image Findings

^{99m}Tc -MIBI

We evaluated 336 segments in 21 patients. The details of early-rest images defect scores of 0, 1, 2, 3, and 4 were 168, 96, 42, 21, and 9 segments, respectively. In all 336 segments; an increase in ^{99m}Tc -MIBI washout was observed in 108 segments. We classified the segments into groups 1, 2, 3, 4, and 5 with 106, 62, 101, 46, and 21 segments, respectively.

Cardiac MRI

LGE regions were observed in 104 segments.

Relationship between ^{99m}Tc -MIBI and cardiac MRI

Table 2 shows the numbers of segments classified according to the presence or absence of ^{99m}Tc -MIBI washout and LGE. No significant association was observed between the presence or absence of ^{99m}Tc -MIBI washout and that of LGE (Fisher's exact test, $p=0.165$).

Table 3 shows the numbers of segments classified according to the defect score in the early-rest images and the presence or absence of LGE. LGE positive counts increased significantly with increase in the defect score segments (Fisher's exact test, $p < 0.001$).

Groups 1 and 2 were classified as normal perfusion of ^{99m}Tc -MIBI. Among the 168 segments classified into groups 1 or 2,

Table 3 Myocardial perfusion defect with early rest images of ^{99m}Tc -MIBI

Defect Score	Numbers n (column %)	LGE (negative)	LGE (positive) n (row %)
0	168 (50%)	139	29 (17.2%)
1	96 (28.5%)	62	34 (35.4%)
2	42 (12.5%)	24	18 (42.8%)
3	21 (6.3%)	5	16 (76.1%)
4	9 (2.7%)	2	7 (77.8%)

defect score; 0: normal uptake, 1: mildly decreased, 2: moderately decreased, 3: severe decreased, 4: perfusion defect
LGE: late gadolinium enhancement
Fisher's exact test: $p < 0.001$.

Table 4 Segments with normal ^{99m}Tc -MIBI perfusion in early rest images

Group	LGE (negative)	LGE (positive)	Total
Group 1	93 (80.2%)	13 (19.8%)	106
Group 2	46 (74.2%)	16 (25.8%)	62

LGE: late gadolinium enhancement
MIBI: ^{99m}Tc -methoxy-isobutyl-isonitrile
Fisher's exact test: $p = 0.033$

Table 5 Segments with ^{99m}Tc -MIBI uptake decrease in early rest images

Group	LGE (negative)	LGE (positive)	Total
Group 3	58 (57.4%)	43 (42.5%)	101
Group 4	23 (50%)	23 (50%)	46

LGE: late gadolinium enhancement
MIBI: ^{99m}Tc -methoxy-isobutyl-isonitrile
Fisher's exact test: $p = 0.475$

washout was observed in 62 segments (36.9%), and LGE regions were observed in 29 segments (17.2%). LGE was significantly more frequent in segments with ^{99m}Tc -MIBI washout than in those without (Fisher's exact test, $p = 0.033$) (Table 4).

Groups 3 and 4 were classified as having decreased ^{99m}Tc -MIBI uptake. Among the 147 segments classified into group 3 or 4, washout was observed in 23 segments (15.6%) and LGE regions in 66 segments (44.8%). There was no significant association between the presence or absence of ^{99m}Tc -MIBI washout and LGE frequency (Fisher's exact test, $p = 0.475$) (Table 5). We presented the typical case of early-stage and advanced cardiomyopathy (Figure 2 and 3).

Discussion

In this study, we investigated the association of ^{99m}Tc -MIBI initial uptake, ^{99m}Tc -MIBI washout, and LGE with MRI. LGE was more frequently observed in segments with decreased ^{99m}Tc -MIBI uptake than those with normal uptake. Furthermore, in the segments without an abnormal ^{99m}Tc -MIBI uptake in early-rest images, a significant association was

observed between increased ^{99m}Tc -MIBI washout and LGE presence.

In previous studies, researchers compared the diagnostic significance of the presence of LGE on cardiac MRI with that of an abnormal pattern of perfusion/metabolism. Those studies reported that the diagnostic ability of LGE is better for patients with moderate or more severe myocardial fibrosis, whereas, for those with the early-stage disorder, evaluation of the perfusion/metabolism mismatch is a more sensitive measurement (11, 19). The results of those studies also indicated that compared with the presence of LGE, the presence of mismatches correlates more closely with the survival rate in patients with cardiomyopathy, suggesting that myocardial evaluation by ^{99m}Tc -MIBI is more sensitive than LGE.

Carvalho et al. have shown that approximately 90% of ^{99m}Tc -MIBI *in vivo* is associated with mitochondria in an energy-dependent manner as a free cationic complex (20). Piwnicka-Worms et al. reported that in the ischemic model, myocardial ^{99m}Tc -MIBI uptake was significantly decreased in cases of mild ischemia and further decreased in cases of severe ischemia (3). Thus, retention of ^{99m}Tc -MIBI in the myocar-

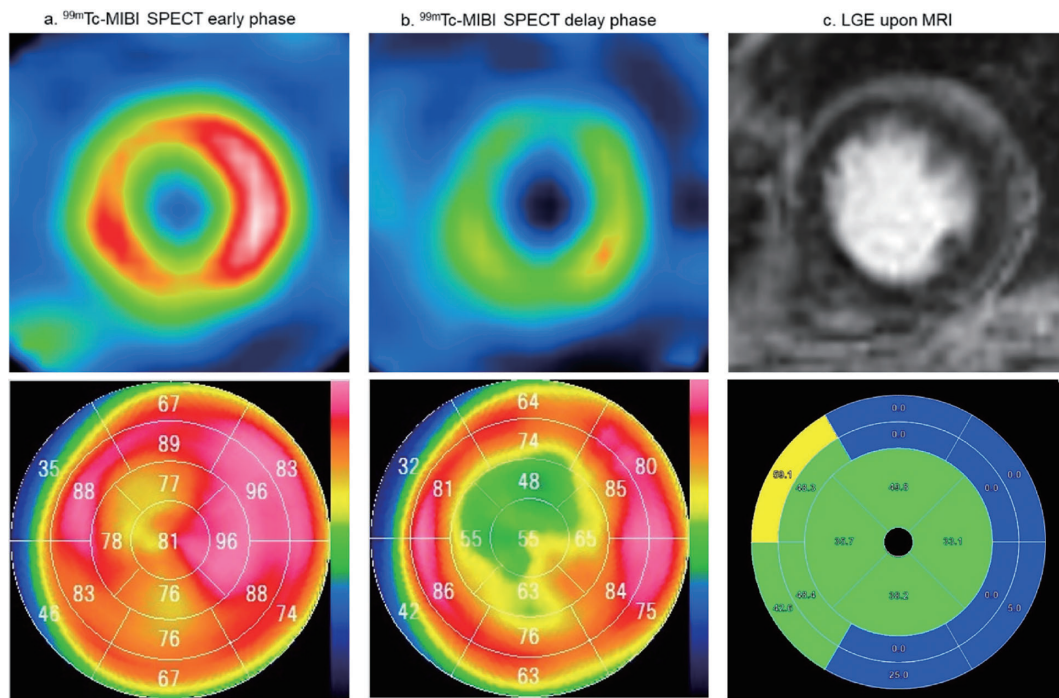


Figure 2 Typical case of early-stage cardiomyopathy. An 81-year-old woman was diagnosed with takotsubo cardiomyopathy. Echocardiogram revealed systolic dysfunction (ejection fraction 46%, end diastolic volume 85 mL, end systolic volume 46 mL). The left ventricular wall motion was severely hypokinetic from the middle to the apex. ^{99m}Tc -MIBI single-photon emission computerized tomography (SPECT) and cardiac magnetic resonance imaging (MRI) were performed within three days. On SPECT, ^{99m}Tc -MIBI uptake was decreased in a small area of the anteroapical and inferior wall. Increased washout in the wide area of the middle to the apex is shown. No late gadolinium enhancement (LGE) is noted.

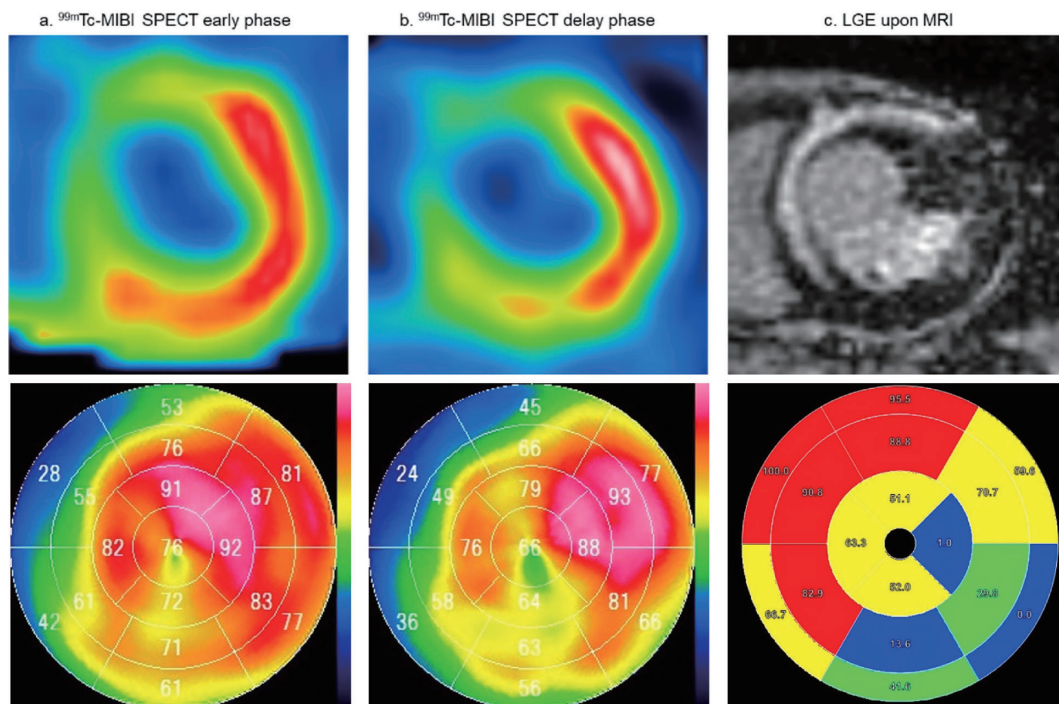


Figure 3 Typical case of advanced cardiomyopathy. A 59-year-old man was diagnosed with cardiac sarcoidosis. Echocardiogram revealed lower normal systolic function (ejection fraction 50%, end diastolic volume 94 mL, end systolic volume 47 mL). The left ventricular wall motion was akinetic from the base to the middle of the anteroapical wall, and mild dyskinesia was observed in the inferior wall. ^{99m}Tc -MIBI single-photon emission computerized tomography (SPECT) and cardiac magnetic resonance imaging (MRI) were performed within three days. On SPECT, ^{99m}Tc -MIBI uptake decreased from the base of the anterior wall to the septum. Increased washout from the middle to the apex of the anterior wall, septum, and the inferior wall is shown. Late gadolinium enhancement (LGE) in a wide area from the anterior wall to the septum and a small area of the inferior wall is shown.

dium is closely related to normal mitochondrial function. Additionally, in the damaged myocardium, impairment in energy production functions and transfer in mitochondria can result in the rapid release of ^{99m}Tc -MIBI (1, 20).

Sekiguchi M et al., in biopsy specimens from the left ventricle of patients with hypertrophic cardiomyopathy, have shown that abnormal giant mitochondria resulted from abnormal metabolic processes in the myocardium (21). Sarai et al. have reported that ^{99m}Tc -MIBI washout correlates with mitochondrial dysfunction in cardiac sarcoidosis (22). Other reports have shown mitochondrial dysfunction occurring in the impaired myocardium of cardiomyopathies (23, 24). A recent report has shown that an increase in the ^{99m}Tc -MIBI washout was correlated with decreased myocardial mitochondrial mRNA expression or an abnormal mitochondrial morphology in patients with dilated cardiomyopathy (DCM). The mRNA of several mitochondrial proteins is involved in myocardial adenosine triphosphate (ATP) production in patients with DCM. Mitochondrial ATP production is mainly generated by the tricarboxylic acid cycle in the mitochondrial matrix and the electron transport chain in the mitochondrial membrane. Electron microscopic findings have shown that the severity of degeneration of mitochondria cristae in the myocardium is correlated with myocardial ^{99m}Tc -MIBI washout (25). An increase in ^{99m}Tc -MIBI washout was observed in heart failure and ischemic patients with low LV ejection fraction and patients with congestive heart failure and low ^{99m}Tc -MIBI uptake (26, 27). Ono et al. reported that an increased ^{99m}Tc -MIBI washout was observed in cases of coronary spastic angina, suggesting that the ability of cardiomyocytes to retain the tracer is impaired in viable but damaged myocardium. They also reported that appropriate treatment improves cardiac function and reduces ^{99m}Tc -MIBI washout (28).

LGE reflects myocardial fibrosis and indicates irreversible and advanced myocardial impairment (7-9, 16). There is a significant overlap between LGE and infarction, as defined by histology (29). Moreover, mitochondrial abnormalities might provoke myocardial fibrotic remodeling and dysfunction through alterations in intracellular calcium signaling. Fibrotic changes in the myocardium are observed in advanced stages of mitochondrial damage. (30, 31). Thus, it has been suggested that mitochondrial dysfunction occurs in cardiomyopathy, and ^{99m}Tc -MIBI washout, abnormal ^{99m}Tc -MIBI uptake, and LGE are observed, depending on the severity of myocardial impairment.

In this study, we classified the segments according to abnormal ^{99m}Tc -MIBI uptake in the early-rest images and washout. Myocardial damage in the segments progressed from groups 1 to 4. Thus, there was a tendency for the frequency of LGE to increase from groups 1 to 4. Even in segments with normal ^{99m}Tc -MIBI uptake in early-rest images, some seg-

ments showed ^{99m}Tc -MIBI washout. These segments should have also had positive LGE. However, LGE frequency in these segments was less than that in segments with ^{99m}Tc -MIBI washout. LGE frequency is associated with a ^{99m}Tc -MIBI uptake and washout. LGE on cardiac MRI is generally recognized as a useful examination to assess the degree of myocardial disorder in cardiomyopathy (6). While evaluating the clinical stage of cardiomyopathy, we observed that as myocardial damage progresses, ^{99m}Tc -MIBI washout increases first, followed by an abnormal ^{99m}Tc -MIBI uptake, with LGE finally appearing. Therefore, adding delayed-rest ^{99m}Tc -MIBI images and washout assessments may provide additional pathophysiological information in patients with cardiomyopathy.

Several limitations are associated with this study. First, this retrospective study was performed at a single institution, and the small sample size did not permit the assessment of the prognostic value of the ^{99m}Tc -MIBI uptake and LGE on MRI in cardiomyopathy. We investigated cardiomyopathy as a whole and have not conducted any disease-specific studies. The correlation of the within-patient segments was not adjusted for in this analysis. This is common in studies with a small population. The gold standard imaging technique for myocardial impairment is LGE, which evaluates fibrosis. In this study, we showed that early- and delayed-rest ^{99m}Tc -MIBI SPECT imaging might be able to assess early myocardial impairment; however, there is insufficient clinical consensus regarding the significance of ^{99m}Tc -MIBI washout. Multimodal imaging may help evaluate the progression of mitochondrial damage in the myocardium, leading to fibrosis. We believe that ^{99m}Tc -MIBI washout reflects early impairment while LGE reflects advanced impairment. However, we did not examine the changes over time, nor their relationship with clinical stage. Furthermore, myocardial impairment, fibrosis, and mitochondrial function were not examined pathologically or immunohistochemically. In this study, the ^{99m}Tc -MIBI uptake abnormality was visually evaluated for all early- and delayed-rest images, and the washout was calculated from the defect score. Since the presence or absence of ^{99m}Tc -MIBI washout was not determined by directly comparing the early- and delayed-rest images, the result may have differed from that of direct evaluation of washout. Additionally, the relationship between the fill-in, which showed an increase in tracer uptake from early to delayed-rest images, and LGE was not evaluated. Segments with ^{99m}Tc -MIBI fill-in (classified as group 5 in this study) were evident in patients with acute myocardial infarction after successful coronary revascularization (2, 32). However, the clinical significance of acquiring images of ^{99m}Tc -MIBI fill-in has not been completely established. The number of segments classified as group 5 was extremely small, and its significance was difficult to evaluate.

To our knowledge, this study is the first to identify the relationship of ^{99m}Tc -MIBI uptake abnormality, ^{99m}Tc -MIBI washout, and LGE with MRI. The evaluation of ^{99m}Tc -MIBI washout by rest perfusion scintigraphy using ^{99m}Tc -MIBI can be performed easily as a routine examination for diagnosing cardiomyopathy. Furthermore, detecting early-stage myocardial impairment by evaluating ^{99m}Tc -MIBI washout may increase the possibility of an early diagnosis of cardiomyopathy and lead to more effective treatments.

Conclusion

An abnormal ^{99m}Tc -MIBI uptake reflects mitochondrial dysfunction. Early and delayed ^{99m}Tc -MIBI SPECT is useful in diagnosing earlier myocardial damage stages, which cannot be detected using the standard one-time acquisition of early-rest ^{99m}Tc -MIBI images. LGE can demonstrate tissue fibrosis in advanced stages of myocardial damage. The severity of myocardial damage and clinical stage of cardiomyopathy can be evaluated using ^{99m}Tc -MIBI early/delayed-rest images and cardiac MRI.

Acknowledgment

The authors are grateful to Keiichiro Yoshinaga MD, PhD, for suggesting helpful advice and performing critical revision. We would like to offer our profound gratitude.

Sources of funding

None.

Conflicts of interest

The authors declare no conflicts of interest.

Reprint requests and correspondence:

Shoichiro Takao, MD, PhD

Department of Diagnostic Radiology, Graduate School of Biomedical Sciences, Tokushima University, 3-18-15 Kuramoto-Cho, Tokushima 770-8509, Japan

E-mail: takao@tokushima-u.ac.jp

References

- Piwnica-Worms D, Kronauge JF, Chiu ML. Uptake and retention of hexakis (2-methoxyisobutyl isonitrile) technetium (I) in cultured chick myocardial cells. Mitochondrial and plasma membrane potential dependence. *Circulation* 1990; 82: 1826–38.
- Takeishi Y, Sukekawa H, Fujiwara S, Ikeno E, Sasaki Y, Tomoike H. Reverse redistribution of technetium-99m-sestamibi following direct PTCA in acute myocardial infarction. *J Nucl Med* 1996; 37: 1289–94.
- Piwnica-Worms D, Chiu ML, Kronauge JF. Divergent kinetics of ^{201}Tl and ^{99m}Tc -SESTAMIBI in cultured chick ventricular myocytes during ATP depletion. *Circulation* 1992; 85: 1531–41.
- Matsuo S, Nakae I, Tsutamoto T, Okamoto N, Horie M. A novel clinical indicator using Tc-99m sestamibi for evaluating cardiac mitochondrial function in patients with cardiomyopathies. *J Nucl Cardiol* 2007; 14: 215–20.
- Matsuo S, Nakajima K, Kinuya S. Evaluation of cardiac mitochondrial function by a nuclear imaging technique using technetium-99m-MIBI uptake kinetics. *Asia Ocean J Nucl Med Biol* 2013; 1: 39–43.
- Mahrholdt H, Wagner A, Judd RM, Sechtem U, Kim RJ. Delayed enhancement cardiovascular magnetic resonance assessment of non-ischaemic cardiomyopathies. *Eur Heart J* 2005; 26: 1461–74.
- Kramer CM. Role of Cardiac MR imaging in cardiomyopathies. *J Nucl Med* 2015; 56 Suppl 4: 39S–45S.
- Simonetti OP, Kim RJ, Fieno DS, Hillenbrand HB, Wu E, Bundy JM, et al. An improved MR imaging technique for the visualization of myocardial infarction. *Radiology* 2001; 218: 215–23.
- Green JJ, Berger JS, Kramer CM, Salerno M. Prognostic value of late gadolinium enhancement in clinical outcomes for hypertrophic cardiomyopathy. *JACC Cardiovasc Imaging* 2012; 5: 370–7.
- Yuki H, Utsunomiya D, Shiraishi S, Takashio S, Sakamoto F, Tsuda N, et al. Correlation of left ventricular dyssynchrony on gated myocardial perfusion SPECT analysis with extent of late gadolinium enhancement on cardiac magnetic resonance imaging in hypertrophic cardiomyopathy. *Heart Vessels* 2018; 33: 623–9.
- Wang L, Yan C, Zhao S, Fang W. Comparison of ^{99m}Tc -MIBI SPECT/ ^{18}F -FDG PET imaging and cardiac magnetic resonance imaging in patients with idiopathic dilated cardiomyopathy: assessment of cardiac function and myocardial injury. *Clin Nucl Med* 2012; 37: 1163–9.
- Masuda A, Yoshinaga K, Naya M, Manabe O, Yamada S, Iwano H, et al. Accelerated ^{99m}Tc -sestamibi clearance associated with mitochondrial dysfunction and regional left ventricular dysfunction in reperfused myocardium in patients with acute coronary syndrome. *EJNMMI Res* 2016; 6: 41.
- Maes F, Collignon A, Vandermeulen D, Marchal G, Suetens P. Multimodality image registration by maximization of mutual information. *IEEE Trans Med Imaging* 1997; 16: 187–98.
- Lin GS, Hines HH, Grant G, Taylor K, Ryals C. Automated quantification of myocardial ischemia and wall motion defects by use of cardiac SPECT polar mapping and 4-dimensional surface rendering. *J Nucl Med Technol* 2006; 34: 3–17.
- Cerqueira MD, Weissman NJ, Dilsizian V, Jacobs AK, Kaul S, Laskey WK, et al. Standardized myocardial segmentation and nomenclature for tomographic imaging of the heart. A statement for healthcare professionals from the Cardiac Imaging Committee of the Council on Clinical Cardiology of the American Heart Association. *Circulation*. 2002; 105: 539–42.
- Kim RJ, Wu E, Rafael A, Chen EL, Parker MA, Simonetti O, et al. The use of contrast-enhanced magnetic resonance imaging to identify reversible myocardial dysfunction. *N Engl J Med* 2000; 343: 1445–53.
- Bondarenko O, Beek AM, Hofman MBM, Kühl HP, Twisk

Imaging of Cardiomyopathy

- JWR, van Dockum WG, et al. Standardizing the definition of hyperenhancement in the quantitative assessment of infarct size and myocardial viability using delayed contrast-enhanced CMR. *J Cardiovasc Magn Reson* 2005; 7: 481–5.
18. Kitabatake A, Tomoike H. Cardiomyopathy: Diagnostic guidelines and commentary. Research Group on Idiopathic Cardiomyopathy, Intractable Disease Research Project of the Japanese Ministry of Health, Labor and Welfare. Sapporo, Karinsha Co., Ltd., 2005. (in Japanese)
 19. Yoshida A, Takano H, Asai K, Yasutake M, Amano Y, Kumita S, et al. Comparison of perfusion-metabolism mismatch in ^{99m}Tc -MIBI and ^{123}I -BMIPP scintigraphy with cardiac magnetic resonance in patients with dilated cardiomyopathy. *J Card Fail* 2013; 19: 445–53.
 20. Carvalho PA, Chiu ML, Kronauge JF, Kawamura M, Jones AG, Holman BL, et al. Subcellular distribution and analysis of technetium-99m-MIBI in isolated perfused rat hearts. *J Nucl Med* 1992; 33: 1516–22.
 21. Sekiguchi M, Konno S. Diagnosis and classification of primary myocardial disease with the aid of endomyocardial biopsy. *Jpn Circ J* 1971; 35: 737–54.
 22. Sarai M, Morimoto S. Washout Rate of ^{99m}Tc -MIBI myocardial scintigraphy in cardiac sarcoidosis. *The Japanese Journal of Sarcoidosis and Other Granulomatous Disorders* 2012; 32: 60–4. (in Japanese)
 23. Chung YW, Kang SM. An experimental approach to study the function of mitochondria in cardiomyopathy. *BMB Rep* 2015; 48: 541–8.
 24. Lee SR, Han J. Mitochondrial mutations in cardiac disorders. *Adv Exp Med Biol* 2017; 982: 81–111.
 25. Hayashi D, Ohshima S, Isobe S, Cheng XW, Unno K, Funahashi H, et al. Increased ^{99m}Tc -sestamibi washout reflects impaired myocardial contractile and relaxation reserve during dobutamine stress due to mitochondrial dysfunction in dilated cardiomyopathy patients. *J Am Coll Cardiol* 2013; 61: 2007–17.
 26. Kumita S, Seino Y, Cho K, Nakajo H, Toba M, Fukushima Y, et al. Assessment of myocardial washout of Tc-99m-sestamibi in patients with chronic heart failure: comparison with normal control. *Ann Nucl Med* 2002; 16: 237–42.
 27. Sugiura T, Takase H, Toriyama T, Goto T, Ueda R, Dohi Y. Usefulness of Tc-99m methoxyisobutylisonitrile scintigraphy for evaluating congestive heart failure. *J Nucl Cardiol* 2006; 13: 64–8.
 28. Ono S, Takeishi Y, Yamaguchi H, Abe S, Tachibana H, Sato T, et al. Enhanced regional washout of technetium-99m-sestamibi in patients with coronary spastic angina. *Ann Nucl Med* 2003; 17: 393–8.
 29. Rehwald WG, Fieno DS, Chen EL, Kim RJ, Judd RM. Myocardial magnetic resonance imaging contrast agent concentrations after reversible and irreversible ischemic injury. *Circulation* 2002; 105: 224–9.
 30. Norton M, Ng AC, Baird S, Dumoulin A, Shutt T, Mah N, et al. ROMO1 is an essential redox-dependent regulator of mitochondrial dynamics. *Sci Signal* 2014; 7: ra10.
 31. Torrealba N, Aranguiz P, Alonso C, Rothermel BA, Lavandero S. Mitochondria in structural and functional cardiac remodeling. *Adv Exp Med Biol* 2017; 982: 277–306.
 32. Fujiwara S, Takeishi Y, Atsumi H, Yamaki M, Takahashi N, Yamaoka M, et al. Prediction of functional recovery in acute myocardial infarction: comparison between sestamibi reverse redistribution and sestamibi/BMIPP mismatch. *J Nucl Cardiol* 1998; 5: 119–27.